

2010

# Dissociative electron attachment in nonplanar chlorocarbons with $\pi^*$ / $\sigma^*$ -coupled molecular orbitals

Kayvan Aflatooni

Fort Hays State University, kaflatoo@fhsu.edu

Gordon A. Gallup

UNL, ggallup1@unl.edu

Paul Burrow

pburrow1@unl.edu

Follow this and additional works at: <http://digitalcommons.unl.edu/physicsburrow>



Part of the [Physics Commons](#)

---

Aflatooni, Kayvan; Gallup, Gordon A.; and Burrow, Paul, "Dissociative electron attachment in nonplanar chlorocarbons with  $\pi^*$  /  $\sigma^*$  -coupled molecular orbitals" (2010). *Paul Burrow Publications*. 35.

<http://digitalcommons.unl.edu/physicsburrow/35>

This Article is brought to you for free and open access by the Research Papers in Physics and Astronomy at DigitalCommons@University of Nebraska - Lincoln. It has been accepted for inclusion in Paul Burrow Publications by an authorized administrator of DigitalCommons@University of Nebraska - Lincoln.

# Dissociative electron attachment in nonplanar chlorocarbons with $\pi^*/\sigma^*$ -coupled molecular orbitals

K. Aflatooni,<sup>a)</sup> G. A. Gallup, and P. D. Burrow<sup>b)</sup>

Department of Physics and Astronomy, University of Nebraska-Lincoln, Lincoln, Nebraska 68588-0111, USA

(Received 6 November 2009; accepted 26 January 2010; published online 4 March 2010)

Total absolute cross sections for the dissociative electron attachment (DEA) process are reported for a series of nonplanar ethylenic and phenylic compounds monosubstituted with  $(\text{CH}_2)_n\text{Cl}$  groups, where  $n=1-4$ . Coupling between the local  $\pi^*$  molecular orbitals provided by the unsaturated moieties and the  $\sigma^*$  (C-Cl) orbital is thus examined as a function of the separation of these groups. In particular, the coupling is viewed from the perspective of the interacting temporary negative ions formed by short lived occupation of these orbitals and their decay into the DEA channel. A theoretical treatment of “remote” bond breaking, presented elsewhere, satisfactorily accounts for DEA in the chloroethylenic compounds presented here and emphasizes not only the delocalization of the coupled anionic wave functions but the importance of their relative phases. The dependence of the cross sections on the vertical attachment energies, measured by electron transmission spectroscopy, is also explored and compared to that found previously in chlorinated alkanes.

© 2010 American Institute of Physics. [doi:10.1063/1.3319751]

## I. INTRODUCTION

To explore the systematic behavior of the dissociative electron attachment (DEA) process,  $e + \text{AB} \rightarrow \text{AB}^{-*} \rightarrow \text{A} + \text{B}^-$ , in halogenated hydrocarbons at low electron energies, it is useful to group compounds by molecular structure. The simplest class consists of saturated compounds, the chloroalkanes, for example, and the DEA cross sections of these molecules<sup>1</sup> have been shown to be dominated by electron attachment into the lowest unoccupied molecular orbital (LUMO) associated with the C-Cl bond, that is, the antibonding C-Cl  $\sigma^*$  orbital.<sup>2</sup> Electron occupation of higher lying C-Cl  $\sigma^*$  orbitals, in the case of polychlorinated alkanes, may also contribute to DEA but to a much smaller degree. In general, the DEA process in these compounds is exothermic, and the potential surface of the temporary anion along the R-Cl separation coordinate is repulsive in the region over which electron attachment can occur, although shallow minima in the potential curves may appear at larger separations owing to charge-dipole interactions.

Unsaturated chlorohydrocarbons comprise a more complex class of compounds possessing low-lying empty orbitals of  $\pi^*$  symmetry, such as those associated with C=C double bonds or aromatic rings, as well as those of C-Cl  $\sigma^*$  character. In the present work, we consider examples such as allyl chloride and benzyl chloride in which the  $\pi^*$  and  $\sigma^*$  orbitals are coupled owing to the nonplanar geometries of the molecules. The  $\pi^*$  and  $\sigma^*$  symmetry designations are used here in a purely local sense to indicate the respective moieties since the orbitals themselves may be strongly mixed. Planar

compounds such as vinyl chloride and chlorobenzene, in which DEA must take place through vibronic mixing of the  $\pi^*$  and  $\sigma^*$  orbitals, fall in a third class and will not be discussed here.

The purpose of the present paper is to report absolute total DEA cross sections for a number of chlorinated compounds belonging to the nonplanar group discussed above and to examine the correlation between the cross sections and the vertical attachment energies (VAEs). The latter measures the most probable electron energy required to inject a free electron into a particular unoccupied molecular orbital. We examine this dependence in the context of extensive work on the chloroalkanes<sup>1</sup> in which we found a strong correlation between the peak values of the DEA cross sections and VAE. We consider two series of compounds in the present work, namely the ethylenic series  $\text{CH}_2 = \text{CH}-(\text{CH}_2)_n-\text{Cl}$ , the  $(n+2)$ -chloro-1-alkenes, and the phenyl-based series  $\text{C}_6\text{H}_5-(\text{CH}_2)_n-\text{Cl}$ , the 1-chloro- $n$ -phenylalkanes, where  $n=1-4$ . These compounds permit a range of separations between the  $\pi^*$ -bearing unsaturated portion and the C-Cl unit on the other end, although the lack of rigidity introduces conformational problems.

The initial work employing DEA as a probe of intramolecular electron transport between remote  $\pi^*$ - and  $\sigma^*$ -bearing moieties was carried out by Pearl *et al.*<sup>3,4</sup> in studies of rigid chloronorborene structures. Underwood-Lemons *et al.*<sup>5</sup> have reported total absolute DEA cross sections for the halo-1-alkene series with Cl and Br substituents, but not the VAEs for the relevant temporary anion states. The most extensive studies on both the phenyl and ethylenic series have been carried out by Modelli and co-workers<sup>6-8</sup> who have reported VAEs measured by electron transmission spectroscopy<sup>9</sup> (ETS) and total *relative* DEA cross sections for these compounds. The latter were determined with respect to that of

<sup>a)</sup>Present address: Department of Physics, Fort Hays State University, Hays, KS 67601-4099.

<sup>b)</sup>Author to whom correspondence should be addressed. Electronic mail: pburrow1@unl.edu. Tel.: (402) 472-2419. FAX: (402) 472-2879.

chlorobenzene by use of a cold-cathode ion gauge measurement of background pressure in the vacuum system while the target gas was in the collision cell. No corrections for relative ion gauge sensitivities were applied. In more recent work, Modelli<sup>10</sup> has extended this work to the bromoalkylbenzenes.

Our experimental studies are accompanied by calculations of the conformations of the chloro compounds and VAEs determined from Hartree–Fock calculations of the virtual orbital energies, using the 6–31G(d) basis set, and semi-empirical scaling described in the text. Finally, we consider the mechanisms leading to the DEA cross sections as interpreted in a recent model study<sup>11</sup> of remote bond breaking by interacting temporary anion states in the chloroalkenes and chloronorbornenes.

## II. EXPERIMENTAL

Experimental studies were carried out on three separate instruments. Each of these has been previously described and only a brief summary is given here. VAEs are determined using ETS as developed by Sanche and Schulz.<sup>9</sup> Our previous studies in the chloroalkanes are described by Aflatooni *et al.*<sup>2</sup>

Total DEA cross sections are measured using the apparatus described by Aflatooni and Burrow.<sup>1</sup> Care was taken to guarantee operation in the linear pressure region. The temperature of the collision cell was typically  $\approx 65$  °C. Pressures were measured on a capacitance manometer maintained at 45 °C and corrected for thermal transpiration. A crossed electron and molecular beam apparatus was also employed<sup>12</sup> to determine the relative energy dependence of the DEA cross section. The energy resolution and performance of this instrument at low energies are superior to that of the total cross section apparatus. Because the dominant negative ion fragment produced in these molecules is  $\text{Cl}^-$  over the range of energies used here, we need not be concerned with mass discrimination effects arising from the transport of the ions to the multichannel plate array where they are counted. Energy scale calibration to within  $\pm 0.05$  eV is carried out in this apparatus using the sharp peak in the negative ion production occurring very near zero energy. In our figures, we have positioned these peaks precisely at zero energy, however, convolution of the sharply varying and asymmetric cross section with the electron beam distribution actually places the peaks approximately 20 meV above zero, depending on energy resolution. All three of the instruments employ trochoidal monochromators<sup>13</sup> for production of the electron beams, with magnetic fields of 75–125 Gauss. We estimate that the total cross section measurements for the DEA peaks occurring above zero energy are accurate to within  $\pm 15\%$ .

## III. RESULTS IN THE CHLOROALKENES

### A. VAEs

We begin with a discussion of the energies of the temporary anion states in these compounds as determined by ETS. Figure 1 shows the derivative with respect to energy of the electron current transmitted through the collision cell as a

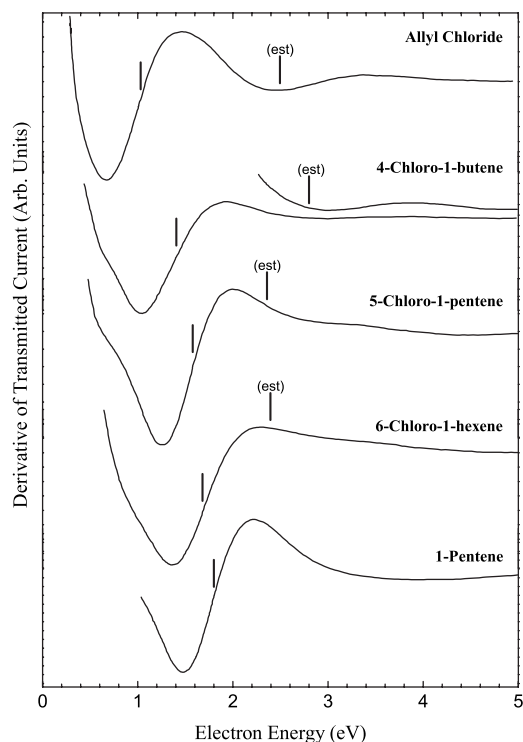


FIG. 1. The derivative with respect to energy of electron beam current transmitted through the chloroalkenes and 1-pentene as a function of electron energy. The vertical bars mark the energies of the midpoints of the features and are associated with the VAEs. The bars labeled “est” (estimated) are located as described in the text.

function of the electron energy. The gas density in the cell was adjusted such that the beam was attenuated by approximately 30%. The presence of a resonance is characterized by a dip and peak in the derivative signal, and the associated VAE is assigned to the energy of the midpoint between these two features and indicated by a vertical line. The spectra of the chloroalkenes exhibit two such structures although clear-cut minima and maxima associated with the upper temporary anion state are only seen in the two shorter compounds. The spectrum of 1-pentene is shown to illustrate the appearance of the  $\pi^*$  temporary anion state in the absence of the C–Cl bond.

In each spectrum, we assign the lower feature to electron occupation of the LUMO of the compound, which is dominated by the C=C  $\pi^*$  molecular orbital but contains a bonding admixture of the C–Cl  $\sigma^*$  orbital. We expect the contribution from the latter to diminish as the separation between the two moieties increases, and as Fig. 1 shows, the first VAE tends toward that of 1-pentene as the compounds increase in length.

Evaluation of the VAE for attachment into LUMO+1 of the chloroalkenes, dominated by the C–Cl  $\sigma^*$  orbital, is more difficult because of the overlap with the C=C  $\pi^*$  resonance and the substantially larger widths of the upper features. We illustrate this problem in Fig. 2 which shows the ET spectra of 1-pentene, ethyl chloride, and a mixture of these two gases. We note that the relative size of the features in the pure compounds is not drawn to the same scale. The energy separation between the dip and peak in the derivative signal is a measure of the width of the resonance and arises from

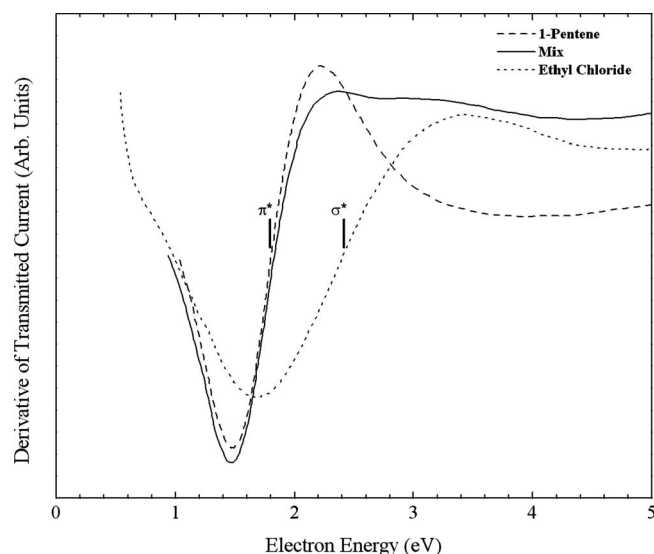


FIG. 2. The derivative of electron beam current transmitted through 1-pentene, ethyl chloride, and a mixture of these two compounds chosen to resemble the results in Fig. 1. The “Mix” data illustrate the way in which the midpoint of the resonance associated with the  $\sigma^*$  (C–Cl) orbital is distorted by the presence of the  $\pi^*$  (C=C) resonance.

broadening owing to the short lifetime of the anion state and from Franck–Condon overlap between the potential surfaces of the ground state of the neutral molecule and that of the anion. The substantially greater width of the C–Cl  $\sigma^*$  resonance in ethyl chloride relative to that of the C=C  $\pi^*$  resonance in 1-pentene is evident.

A “synthetic” ET spectrum for a chloroalkene was devised with a mixture of 1-pentene and ethyl chloride in the collision cell. The relative pressures were adjusted to create a spectrum that resembles that of the longer chloroalkenes in Fig. 1. The key features to note are that the energy of the narrow lower resonance in the mixed gases is essentially unperturbed from that of 1-pentene by the presence of the ethyl chloride  $\sigma^*$  resonance. Second, although the dip and midpoint of the  $\sigma^*$  resonance of ethyl chloride are completely obscured, the small *peak* in the derivative signal of the mixture remains relatively close to that of ethyl chloride.

From our previous ETS studies in the chloroalkanes,<sup>2</sup> we observed that in the monochloroalkanes, the dip and peak energies each vary linearly with VAE. In particular, we found

that  $E_{\text{peak}} = 1.4 * \text{VAE}$ . In the present work, we will assume that this relationship also holds for the predominantly C–Cl  $\sigma^*$  anion states of the chloroalkenes, and we derive *estimated* VAEs for the upper resonance from a measurement of  $E_{\text{peak}}$  by this means. These values are indicated by the vertical lines in Fig. 1 labeled “est.” Needless to say, the estimated value in 6-chloro-1-hexene, in which even the peak in the derivative is not readily discernable, is problematic. Nevertheless, the estimated LUMO+1 VAEs of the longer chloroalkenes approach those (2.23–2.26 eV) found by direct measurement in 1-chloropentane<sup>14</sup> and 1-chlorooctane and 1-chlorononane.<sup>15</sup> As seen in Fig. 1, the trend of LUMO+1 VAEs from allyl chloride to 6-chloro-1-hexene is not monotonic. We show below that this is a consequence of the presence of rotamers in 4-chloro-1-butene with rather different calculated VAEs. These species also account for the greater apparent width of the lowest anion state in this compound. Table I summarizes the LUMO and LUMO+1 VAEs (Ref. 16) and lists the dip to peak energy separation,  $E_{\text{dp}}$ , as well. Agreement with the VAEs determined elsewhere for the lowest anion states in allyl chloride<sup>7</sup> (3-Cl-1-propene) and in 5-chloro-1-pentene<sup>8</sup> is within 30 meV. The estimated VAEs for the LUMO+1 anion states lie below those reported elsewhere, which have not been compensated for overlap with the lowest anion resonance.

## B. Molecular conformations

Underwood-Lemons *et al.*<sup>5</sup> have previously reported geometry optimization calculations for allyl chloride, 4-chloro-1-butene, and 5-chloro-1-pentene using the 6–31G(d) basis set and the GAMESS program. Modelli<sup>8</sup> has also calculated and discussed the role of conformations in the chloroalkenes. In connection with our remote bond breaking model,<sup>11</sup> we have carried out similar calculations on these molecules and the three most prevalent rotamers of 6-chloro-1-hexene. Table II summarizes the various rotamers, their relative energies with respect to that of the lowest energy conformation and the populations at 338 K.

The notation for rotamers is not standardized. We distinguish them by giving approximate dihedral angles along the chain, starting at the  $\text{CH}_2=\text{CH}-$  end. In these compounds, the angles are all close to one of the angles  $0^\circ$ ,  $60^\circ$ ,  $120^\circ$ ,  $180^\circ$ ,  $240^\circ$ , or  $300^\circ$ . Our designations are also the approxi-

TABLE I. VAEs (eV) for the two lowest temporary anion states of the chloroalkenes as measured by ETS. The dip-to-peak separation,  $E_{\text{dp}}$ (eV), of the lowest state is also given. VAEs for the lowest anion states of two comparison molecules are also included.

Compound	LUMO VAE	LUMO $E_{\text{dp}}$	LUMO+1 VAE
3-Cl-1-propene ( $\text{H}_2\text{C}=\text{CH}-\text{CH}_2\text{Cl}$ )	1.04, 1.01 <sup>a</sup>	0.79, 0.85 <sup>a</sup>	2.49(est), 3.14 <sup>b</sup>
4-Cl-1-butene ( $\text{H}_2\text{C}=\text{CH}-(\text{CH}_2)_2\text{Cl}$ )	1.40	0.93	2.8(est)
5-Cl-1-pentene ( $\text{H}_2\text{C}=\text{CH}-(\text{CH}_2)_3\text{Cl}$ )	1.58, 1.60 <sup>b</sup>	0.72	2.35(est), 3.1 <sup>b</sup>
6-Cl-1-hexene ( $\text{H}_2\text{C}=\text{CH}-(\text{CH}_2)_4\text{Cl}$ )	1.68	0.9	2.4(est)
1-pentene ( $\text{H}_2\text{C}=\text{CH}-(\text{CH}_2)_2\text{CH}_3$ )	1.80	0.74	...
1-Cl-pentane ( $\text{CH}_3-(\text{CH}_2)_4\text{Cl}$ )	...	...	2.26 <sup>c</sup>

<sup>a</sup>Reference 7.

<sup>b</sup>Reference 8.

<sup>c</sup>Reference 14.

TABLE II. Angular designations, relative energies, degeneracies, and populations of chloroalkene rotamers at 338 K.

Compound	a1	a2	a3	a4	Energy (meV)	Degen.	Population
3-Cl-1-propene	240				0.0	2	0.928
	0				54.4	1	0.072
4-Cl-1-butene	240	180			0.0	2	0.540
	240	300			22.0	2	0.254
	240	60			39.3	2	0.140
	0	180			49.9	1	0.049
	0	60			100.5	2	0.017
5-Cl-1-pentene	240	60	180		0.0	2	0.226
	240	180	180		1.54	2	0.214
	240	60	60		4.22	2	0.195
	240	180	60		12.02	2	0.149
	240	180	240		14.40	2	0.138
	0	180	180		40.13	1	0.028
	240	240	60		43.59	2	0.051
6-Cl-1-hexene	240	180	180	180	0.00	2	1.0 (Rel.)
	240	180	180	300	13.76	2	0.625 (Rel.)
	240	180	180	60	16.13	2	0.585 (Rel.)

mate dihedral angles that would appear in the well-known Z-matrix method<sup>17</sup> for specifying molecular geometry. Specifically, using I, J, K, and L to represent four atoms in a chain, we give the approximate dihedral angles between the half-planes I-J-K and J-K-L, where J-K is the line common to the two of them. The angles are made unique by using the convention that, looking along J to K, the angle is positive if the J-K-L plane is rotated counterclockwise from the I-J-K plane.

We have not attempted to analyze the rotamers of the 6-chloro-1-hexene compound. However, based on the geometries of the shorter compounds, we have selected three structures that are expected to have low energies. These are 240–180–180– $\varphi$  with  $\varphi=180, 60,$  and  $300$ . As seen in the table, the three selected rotamers have energies well within kT at 338 K. The energies of the rotamers of the chlorobutene and chloropentene compounds are in good agreement with those computed by Underwood-Lemons *et al.*<sup>5</sup>

### C. Calculated VAEs

To compare with our experimental measurements of VAE, we have calculated the first two virtual orbital energies of each of the rotamers given in Table II. These orbital energies can be associated with anion state energies through Koopmans' theorem (KT).<sup>18</sup> Such energies are well known to be incorrect in an absolute sense, although the relative values are more meaningful. By shifting and scaling virtual orbital energies empirically to agree with VAE measurements in a group of related compounds, predicted VAEs may be obtained that are generally in close agreement with experiment.<sup>19,20</sup> For the present work involving alkenes and the phenyl groups discussed later, we employ the scaling  $\text{VAE}=0.753E_{\text{KT}}-1.968$ , determined from ETS measurements in benzene, pyridine, pyrimidine, and naphthalene and

Hartree–Fock calculations with the 6–31G(d) basis set used for both geometry optimization and virtual orbital energies,  $E_{\text{KT}}$ .<sup>21</sup> All the terms are given in eV.

For the second anion state, having mostly  $\sigma^*$  (C–Cl) character, we employ parameters giving  $\text{VAE}=0.90E_{\text{KT}}-2.55$ , obtained from an empirical fit to measured VAEs in a series of chloroalkanes by Aflatooni *et al.*<sup>2</sup> The 6–31G(d) basis set is used for both the geometry optimization and calculation of virtual orbital energies. Table III summarizes the calculated virtual orbital energies (labeled KT) and the empirically scaled values, obtained from the relationships given above, for the two lowest temporary anion states in each of the rotamers. For convenience of comparison, we list the experimental VAEs for both anion states next to those of each of the rotamers.

The trends in the calculated VAEs are generally in agreement with the experimental results in the chloroalkenes and the two comparison molecules 1-chloro-pentane and 1-pentene (Table I), although the spread in values owing to the various rotamers within a given compound make this less transparent. The most striking feature appears in 4-chloro-1-butene in which the most stable rotamer (240–180) exhibits a substantially greater coupling between the  $\pi^*$  and  $\sigma^*$  moieties than found in the next two higher energy rotamers. The calculations predict a spread of 0.35 eV in the energies of the anion state associated with filling the LUMO and 0.47 eV in the spread associated with the LUMO+1, arising from the different rotamers. This result is borne out in a qualitative sense in the ET data shown in Fig. 1. The spread in energy of the lowest anion state of 4-Cl-1-butene, as measured by the dip-to-peak energy separation  $E_{\text{dp}}$  given in Table I, is approximately 0.2 eV larger than that found in the reference molecule 1-pentene and in 5-Cl-1-pentene and allyl chloride. The lowest anion state of 6-Cl-1-hexene also displays additional breadth, but because only three rotamers were investigated in the calculations, the contributors to this width are

TABLE III. KT, scaled KT, and ETS energies of negative ion states. Energies are in eV and geometries are optimized at the 6-31G(d) level.

Compound	Conformation	Anion state	KT	Scaled KT <sup>a</sup>	Expt.
3-Cl-1-propene		LUMO	4.1171	1.132	1.04
		LUMO+1	5.8015	2.68	2.49 (est)
4-Cl-1-butene	240-180	LUMO	4.2967	1.267	1.40
		LUMO+1	5.9974	2.85	2.80 (est)
	240-300	LUMO	4.7593	1.615	1.40
		LUMO+1	5.4722	2.38	2.80 (est)
		LUMO	4.7620	1.617	1.40
5-Cl-1-pentene	240-60	LUMO	5.6164	2.51	2.80 (est)
		LUMO+1	4.7239	1.589	1.58
	240-60-180	LUMO	5.4096	2.32	2.35
		LUMO+1	4.8608	1.699	1.58
	240-180-180	LUMO	5.3089	2.23	2.35
		LUMO+1	4.8110	1.654	1.58
	240-60-60	LUMO	5.6464	2.54	2.35
		LUMO+1	4.9933	1.791	1.58
		LUMO	5.3933	2.31	2.35
		LUMO+1	4.9606	1.767	1.58
6-Cl-1-hexene	240-180-240	LUMO	4.9606	1.767	1.58
		LUMO+1	5.4123	2.33	2.35
	240-180-180-180	LUMO	4.8790	1.705	1.68
		LUMO+1	5.4069	2.32	2.4(est)
	240-180-180-300	LUMO	4.8300	1.669	1.68
		LUMO+1	5.4858	2.39	2.4(est)
	240-180-180-60	LUMO	5.0559	1.839	1.68
		LUMO+1	5.4178	2.33	2.4(est)

<sup>a</sup>LUMO( $\pi^*$ ) scaled as  $VAE=0.753E_{KT}-1.968$ . LUMO+1( $\sigma^*$ ) scaled as  $VAE=0.90E_{KT}-2.55$ .

less certain. It may arise simply from the closer proximity of the two resonances in this compound and overlap of the peak of the lower feature with the dip in the upper. We return to a discussion of the relative splittings between LUMO and LUMO+1 in allylchloride and 4-chloro-1-butene later in the paper.

#### D. DEA cross sections

In Figs. 3(a)–3(d), we show the total cross sections for the DEA process in the chloroalkenes as a function of electron impact energy. The two vertical lines in each panel show the energies of the temporary anion states derived from our ETS measurements. Sharp peaks occur at nominally zero energy in all of the compounds. These are likely to arise from thermally populated vibrationally excited levels of the molecules and from possible contributions from impurities such as  $CCl_4$  and will not be considered further here. Rather, our focus will be on the roughly symmetric peaks lying just below the first VAE. The magnitudes and energies of these peaks as determined in the present work and by Underwood-Lemons *et al.*<sup>5</sup> are given in Table IV. Relative DEA cross sections for allyl chloride<sup>7,8</sup> and 5-chloro-1-pentene<sup>8</sup> with respect to that of chlorobenzene have been determined by Modelli and co-workers.<sup>6-8</sup> The cross section ratios are obtained assuming that the ion gauge sensitivity is the same in each of the compounds. We have placed these relative values on an absolute scale using our recently measured value for the peak DEA cross section of chlorobenzene of  $2.35 \times 10^{-17} \text{ cm}^2$  and listed them also in Table IV.

Agreement between the present work and that of Underwood-Lemons *et al.*<sup>5</sup> for allyl chloride (3-chloro-1-propene) is excellent. In the remaining compounds, however, there is substantial disagreement, with the cross sections of Underwood-Lemons *et al.*<sup>5</sup> lying above those of the present

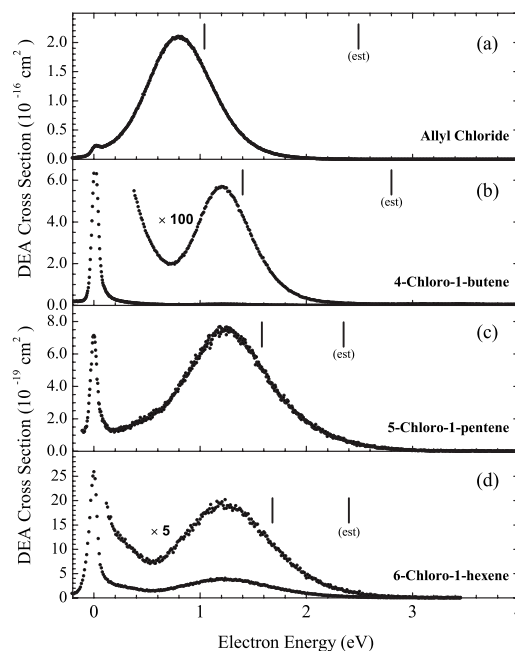


FIG. 3. The DEA cross section of (a) allyl chloride, (b) 4-chloro-1-butene, (c) 5-chloro-1-pentene, and (d) 6-chloro-1-hexene as a function of electron energy. The vertical bars indicate the positions of the two lowest resonances as determined by ETS.

TABLE IV. Peak DEA cross sections ( $\text{cm}^2$ ) and energies of the peaks (eV) in the n-chloro-1-alkenes.

Compound	Reference	Peak cross section	Peak energy
3-Cl-1-propene	Present work	$2.10 \times 10^{-16}$	0.81
	Ref. 5	$2.38 \times 10^{-16}$	0.97
	Refs. 7 and 8	$1.51 \times 10^{-16a}$	0.79
4-Cl-1-butene	Present work	$5.70 \times 10^{-18}$	1.20
	Ref. 5	$1.48 \times 10^{-17}$	1.37
5-Cl-1-pentene	Present work	$7.54 \times 10^{-19}$	1.24
	Ref. 5	$1.3 \times 10^{-18}$	1.30
	Ref. 8	$6.8 \times 10^{-19a}$	1.5
6-Cl-1-hexene	Present work	$4.03 \times 10^{-19}$	1.23
	Ref. 5	$1.0 \times 10^{-18}$	1.26

<sup>a</sup>Obtained from ratios normalized to a chlorobenzene DEA cross section of  $2.35 \times 10^{-17} \text{ cm}^2$ .

work by factors of 2.6, 1.7, and 2.5, respectively, in the successively longer compounds. The reasons for the discrepancies are not known. The two cross sections inferred from the relative values of Modelli and co-workers<sup>7,8</sup> are in rather good agreement with the present work considering the method of normalization, lying 28% lower in allyl chloride and 10% lower in 5-chloro-1-pentene.

#### IV. DISCUSSION OF N-CHLORO-1-ALKENES

In this section, we consider in more detail the variation of the peak DEA cross sections with various properties of the chloroalkene compounds, in particular, the dependence on VAE. For this purpose, it is convenient to consider our results in conjunction with those from our earlier study of the chloroalkenes.<sup>1</sup> The most significant outcome of that work showed a strong correlation between peak DEA cross section and VAE. This is recalled here in Fig. 4 in which the peak

cross sections of approximately 40 chloroalkanes are plotted versus VAE on a semilog scale. Specific information about these data may be found in the original references.<sup>1,2</sup> In brief, a best-fit line was fit to the data over the range from 0.6 to 2.8 eV. Extension of this line to 3.4 eV was found to be in good agreement with the cross section computed by Fabrikant<sup>22</sup> for the  $v=0$  vibrational level of  $\text{CH}_3\text{Cl}$ . The correlation with VAE thus extends over almost seven orders of magnitude in peak cross section. Only one significant departure from the curve was found, that for  $\text{CH}_2\text{Cl}_2$ , not shown in Fig. 4, which lies a factor of  $\approx 20$  below the line at its VAE of 1.01 eV. The scatter in the remaining compounds averages 38% from the best-fit line. As discussed elsewhere,<sup>1</sup> the correlation arises because of the close “family” resemblance of the anion states of these compounds, leading to a monotonic variation in the lifetimes of the temporary anion states with VAE and in the times required for the R–Cl nuclei to separate to a distance where autodetachment of the additional electron can no longer take place.

The chloroalkane data in Fig. 4 provide a useful template on which to visualize the effects of coupling between the  $\pi^*$  and  $\sigma^*$  anion states and to place the DEA magnitudes relative to those of the saturated compounds bearing only empty  $\sigma^*$  orbitals. We have plotted the peak DEA cross section of each chloroalkene at *both* the VAE corresponding to the LUMO (nominally  $\pi^*$ ) resonance, filled star symbol, as well as the VAE of the LUMO+1 (nominally  $\sigma^*$ ) resonance, open star symbol. In Fig. 4, the numbers 1–4 refer to the number of  $\text{CH}_2$  groups separating the C=C and C–Cl moieties. Straight lines are drawn between the points only to guide the eye.

As the bridge connecting the C=C and C–Cl groups increases in length, the peak DEA cross sections decline in an apparently exponential manner as a function of the LUMO VAE, falling below the best-fit chloroalkane line by steadily increasing amounts. The VAEs of the lower resonance shift to higher energy, reflecting the reduced mixing with the upper anion state. In the limit of complete decoupling between the ends, we would expect the VAE to reach a value typical of the  $\pi^*$  anion state of a long normal alkene. For illustration, the  $\pi^*$  VAE for 1-pentene at 1.80 eV is indicated in Fig. 4 by a vertical dashed line. The LUMO VAE of 6-Cl-1-hexene lies 0.12 eV below that of 1-pentene, suggesting that some coupling still exists. This is consistent also with the KT calculations for these compounds.

The DEA cross sections plotted at the LUMO+1 VAEs of allyl chloride (1) and 4-chloro-1-butene (2), open stars, serve only to illustrate that the cross sections are orders of magnitude larger than those of the saturated compounds with comparable values of VAE. However, in the two longest compounds, (3) and (4), the cross sections lie only a factor of three above the best fit line for the chloroalkanes, and their LUMO+1 VAEs are approaching a value close to that for longer mono-chloroalkanes such as 1-chloro-pentane, whose VAE is shown by the vertical dashed line at 2.26 eV.<sup>14</sup> The evidence presented in Fig. 4 thus suggests that even in 6-chloro-1-hexene there still remains enough coupling between the C=C and C–Cl moieties to affect the DEA cross section.

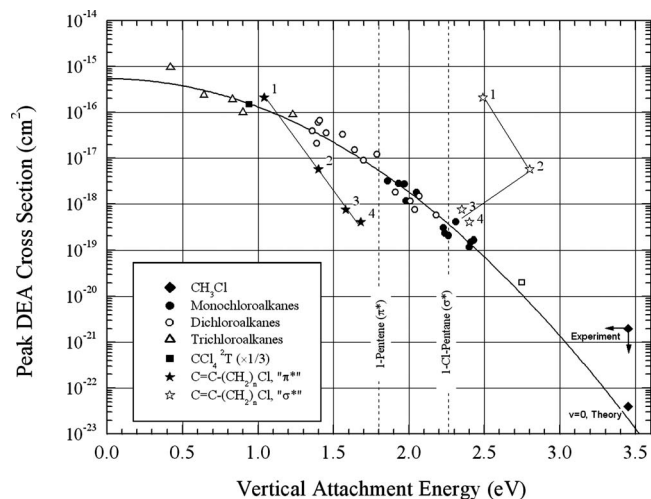


FIG. 4. The peak DEA cross section for a series of mono- and polychloroalkanes as a function of electron energy and a best-fit line through these data taken from Ref. 1. (See this reference also for the open square data point.) The open and filled stars show the DEA cross sections for the chloroalkenes measured here and plotted at both the lower, primarily  $\pi^*$  VAE, and upper, primarily  $\sigma^*$  VAE. With increasing numbers of  $(\text{CH}_2)$  spacer groups, the DEA cross section is observed to approach the line characteristic of the chloroalkanes, as the VAEs approach the values typical of the separated moieties.

Allyl chloride has by far the largest DEA cross section of this set of molecules, however, the mixing between the  $\pi^*$  (C=C) and  $\sigma^*$  (C-Cl) moieties, as judged by the splitting between the LUMO and LUMO+1 anion states, is essentially the same as that of the lowest conformer of 4-chloro-1-butene, as seen in the scaled KT energies and in the experimental energies in Table III. It may therefore be puzzling that the DEA cross section of allyl chloride is 37 times larger, given that the most stable conformer of 4-chloro-1-butene makes up 54% of the total population of the latter compound.

The answer to this question in part can be found in the model DEA study of Burrow and Gallup.<sup>11</sup> In brief, this treatment derived an expression for the lifetime of a “composite” resonance made up from the mixing of temporary anion states belonging to two separate moieties, namely an unsaturated ethylenic component and a saturated group containing the C-Cl bond. The lifetime can be expressed in terms of the lifetimes of the unmixed resonances and certain wave function coefficients and signs that can be computed quantum chemically. Using empirical values for the VAEs and lifetimes of the *unmixed* resonances, along with a simplified relationship between lifetime and DEA cross section, the DEA cross sections for the compounds discussed here and two other rigid chloronorborenes was predicted and found to be in satisfactory agreement with experiment.

The analysis<sup>11</sup> showed that the LUMO resonance of allyl chloride possesses a substantially longer lifetime than that of the most stable conformer of 4-chloro-1-butene, thus accounting for its much larger DEA cross section. The source for this arises in part from a rather subtle cancellation owing to a sign difference occurring in the expression for the composite resonance width. In essence, there is an interference in the electron wave functions of the two anionic moieties as they decay into the continuum.

## V. RESULTS IN 1-CHLORO-N-PHENYLALKANES

### A. VAEs

The VAEs of the  $C_6H_5-(CH_2)_n-Cl$  compounds have been determined using ETS for  $n=1$  (benzyl chloride) by Stricklett *et al.*<sup>16</sup> and Distefano *et al.*,<sup>23</sup> and for  $n=2-4$  by Modelli and co-workers,<sup>6,7</sup> and in the present work. As in the chloroethenes, the  $\pi^*$  resonances are very prominent, and there is some concern that the VAEs associated with the C-Cl  $\sigma^*$  resonances could be distorted by their proximity. We illustrate this in Fig. 5, showing ETS data in 1-phenylhexane, ethyl chloride, and a mix of the two gases reflecting the approximate sizes of the resonances as observed in the  $C_6H_5-(CH_2)_n-Cl$  compounds. Again it is observed that the “dip” associated with the  $\sigma^*$  resonance is strongly overlapped by the “peak” in the  $\pi^*$  resonances appearing near 1.5 eV, and thus, the apparent midpoint of the  $\sigma^*$  resonance as read from the mixture data will fall above that of the isolated resonance. Furthermore the  $\sigma^*$  resonance appears to be much narrower.

In the chloroethenes, we used a crude means to compensate for the  $\pi^*$  resonance overlap, namely, taking the energy

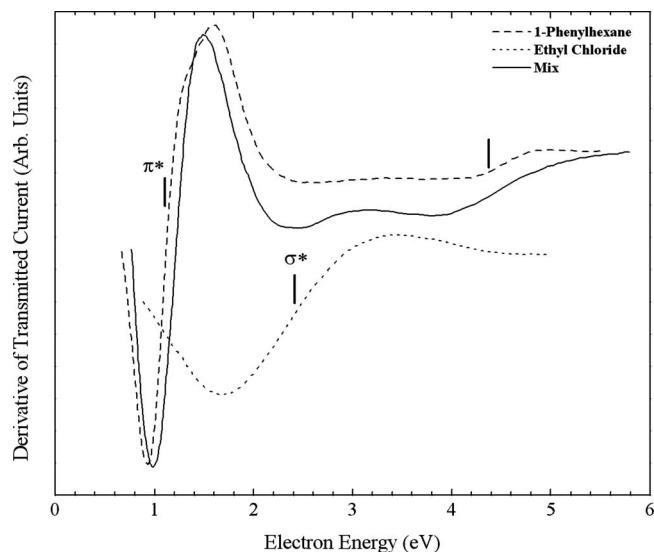


FIG. 5. As shown in Fig. 2 for 1-phenylhexane, ethyl chloride, and a mixture of these compounds.

of the positive maximum of the  $\sigma^*$  resonance in the ET spectrum and dividing by 1.4, as found in our earlier work in the chloroalkanes. Unfortunately, Fig. 5 also indicates that the position of the maximum is depressed somewhat by the dip associated with the  $\pi_3^*$  resonance appearing near 4.5 eV. We will again cite these estimated values for  $\sigma^*$  VAEs but note that in the phenylchloroalkanes these values may be lower bounds.

Table V summarizes the VAEs of these compounds for the lowest  $\pi_1^*$  and  $\sigma^*(C-Cl)$  resonances. The present values for the  $\sigma^*$  resonances are labeled “est” and have been derived as described above. Readers are referred to Refs 6, 7, 16, and 23 for the ET spectra. We omit any discussion of the  $\pi_2^*$  orbitals that derive from the degenerate  $e_{2u}$  orbital of benzene as these have a node where the chloroalkyl groups attach and are not expected to contribute appreciably to the DEA cross section in these compounds.

### B. Calculated conformers and VAEs

Table VI summarizes the relative energies of the stable conformations of the phenylchloroalkanes and the populations at 338K as computed with a 6-31G(d) basis set. The conformer energies differ somewhat from those of Modelli *et al.*<sup>7</sup> who used DFT/B3LYP calculations with the same basis set. The most stable conformation of  $C_6H_5-(CH_2)_3Cl$  also

TABLE V. VAEs in eV as measured by ETS for the lowest  $\pi^*$  and  $\sigma^*$  anion states of the 1-chloro-n-phenylalkanes.

Compound	LUMO( $\pi_1^*$ ) VAE	LUMO+2( $\sigma^*$ ) VAE
$C_6H_5-CH_2Cl$ (benzyl chloride)	0.63, <sup>a</sup> 0.65 <sup>b</sup>	2.86, <sup>a</sup> 2.8 <sup>b</sup> , 2.58(est)
$C_6H_5-(CH_2)_2Cl$	0.87, <sup>c</sup> 0.89	2.7, <sup>c</sup> 2.5(est)
$C_6H_5-(CH_2)_3Cl$	0.95, <sup>d</sup> 0.97	2.65, <sup>d</sup> 2.4(est)
$C_6H_5-(CH_2)_4Cl$	1.00, <sup>d</sup> 1.00	2.6, <sup>d</sup> 2.34(est)

<sup>a</sup>Reference 16.

<sup>b</sup>Reference 23.

<sup>c</sup>Reference 6.

<sup>d</sup>Reference 7.



TABLE VI. Angular designations, relative energies, degeneracies, and populations of phenylchloroalkane rotamers at 338 K.

Compound	a1	a2	a3	a4	Degen.	Energy (meV)	Population
C <sub>6</sub> H <sub>5</sub> -(CH <sub>2</sub> )Cl	90				1	0.0	1.0
C <sub>6</sub> H <sub>5</sub> -(CH <sub>2</sub> ) <sub>2</sub> Cl	90	180			1	0.0	0.811
	90	60			2	62.7	0.189
C <sub>6</sub> H <sub>5</sub> -(CH <sub>2</sub> ) <sub>3</sub> Cl	90	180	180		1	0.0	0.171
	90	60	60		2	2.07	0.318
	90	180	60		2	4.57	0.292
	90	60	180		2	13.0	0.218
C <sub>6</sub> H <sub>5</sub> -(CH <sub>2</sub> ) <sub>4</sub> Cl	90	60	300		2	181	0.001
	90	180	180	180	1	0.0	1.00 (Rel.)
	90	180	180	60	2	21.0	0.973 (Rel.)

differs but we have not pursued this further. Table VII lists the KT and scaled KT energies for each of the stable conformers. The right hand column lists the experimental energies for each compound as determined by ETS. The VAEs are repeated for each conformer for comparison.

The scaled KT values emulate the trends observed in the experimental  $\pi_1^*$  VAEs rather well, although in the two shortest compounds the scaled values lie approximately 0.13 eV below experiment. The scaled  $\sigma^*$  (C-Cl) energies are in very good agreement with the experimental values marked (est), showing the importance of accounting for overlap with the  $\pi^*$  resonances.

### C. DEA cross sections

Figures 6(a)–6(d) illustrates the total cross sections for the DEA process in the phenylchloroalkanes as a function of electron impact energy. As in Fig. 3, the vertical lines indi-

cate the energies of the temporary anion states derived from our ETS measurements. Similar to the chloroalkene compounds, sharp peaks are observed at nominally zero energy which we will not consider further. The magnitudes and energies of the DEA peaks lying near the lowest VAE are given in Table VIII. To our knowledge, there are no other absolute measurements with which to compare. However, relative values given by Modelli and co-workers<sup>6,7</sup> can be put on an absolute scale by reference to the DEA cross section of chlorobenzene, as indicated earlier for the chloroalkenes, and these values are also included in Table VIII. Except for C<sub>6</sub>H<sub>5</sub>-(CH<sub>2</sub>)<sub>4</sub>-Cl, they fall within  $\pm 45\%$  of the present cross sections. For the longest compound, having the smallest cross section, the difference is 100%.

We note that the DEA cross section of C<sub>6</sub>H<sub>5</sub>-(CH<sub>2</sub>)<sub>4</sub>-Cl, as seen in Fig. 6(d), shows a relatively small peak that appears to lie on a background of unknown

TABLE VII. KT, scaled KT, and ETS energies of phenylchloroalkane temporary anion states. Energies are in eV and geometries are optimized at the HF 6-31G(d) level.

Compound	Conformation	Anion State	KT	Scaled KT <sup>a</sup>	Expt.
C <sub>6</sub> H <sub>5</sub> -(CH <sub>2</sub> )Cl	90	LUMO( $\pi_1^*$ )	3.2871	0.5068	0.64 <sup>b</sup>
		LUMO+2( $\sigma^*$ )	5.7797	2.6574	2.6 (est)
C <sub>6</sub> H <sub>5</sub> -(CH <sub>2</sub> ) <sub>2</sub> Cl	90-180	LUMO( $\pi_1^*$ )	3.5973	0.7403	0.89
		LUMO+2( $\sigma^*$ )	5.6164	2.5103	2.5 (est)
C <sub>6</sub> H <sub>5</sub> -(CH <sub>2</sub> ) <sub>3</sub> Cl	90-60	LUMO( $\pi_1^*$ )	3.8341	0.9186	0.89
		LUMO+2( $\sigma^*$ )	5.5375	2.4392	2.5 (est)
	90-180-180	LUMO( $\pi_1^*$ )	3.8776	0.9514	0.97
		LUMO+2( $\sigma^*$ )	5.3171	2.2406	2.4 (est)
90-60-60	LUMO( $\pi_1^*$ )	3.8368	0.9206	0.97	
	LUMO+2( $\sigma^*$ )	5.5593	2.4588	2.4 (est)	
	90-180-60	LUMO( $\pi_1^*$ )	3.9402	0.9985	0.97
		LUMO+2( $\sigma^*$ )	5.4015	2.3166	2.4 (est)
90-60-180	LUMO( $\pi_1^*$ )	3.7361	0.8448	0.97	
	LUMO+2( $\sigma^*$ )	5.3525	2.2725	2.4 (est)	
	90-60-300	LUMO( $\pi_1^*$ )	3.9974	1.0415	0.97
		LUMO+2( $\sigma^*$ )	5.5266	2.4294	2.4(est)
C <sub>6</sub> H <sub>5</sub> -(CH <sub>2</sub> ) <sub>4</sub> Cl	90-180-180-180	LUMO( $\pi_1^*$ )	3.9184	0.9821	1.00
		LUMO+2( $\sigma^*$ )	5.3389	2.2602	2.3 (est)
		LUMO( $\pi_1^*$ )	4.0110	1.0518	1.00
	90-180-180-60	LUMO+2( $\sigma^*$ )	5.4232	2.3362	2.3 (est)

<sup>a</sup> $\pi_1^*$  KT values scaled with VAE=0.753  $E_{KT}$ -1.968.  $\sigma^*$  KT values scaled with VAE=0.90 $E_{KT}$ -2.55.

<sup>b</sup>Average of results from Refs. 16 and 23.

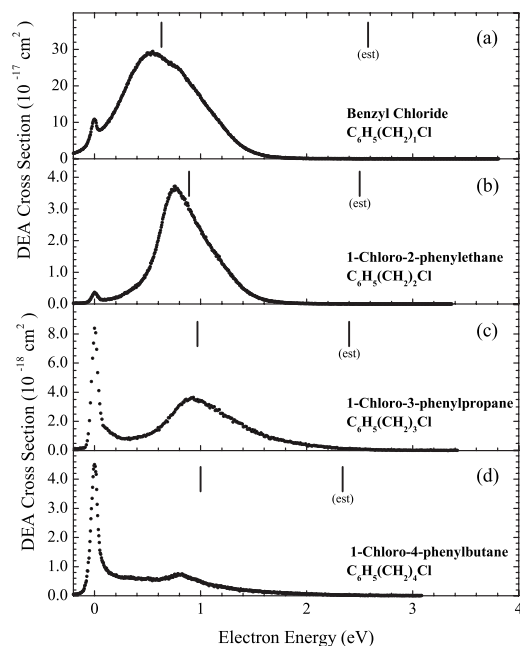


FIG. 6. The DEA cross section of (a) benzyl chloride, (b) 1-chloro-2-phenylethane, (c) 1-chloro-3-phenylpropane, and (d) 1-chloro-4-phenylbutane as a function of electron energy.

origin. We have cited in Table VIII the full height of the peak, however, this likely corresponds to an upper bound for the cross section.

## VI. DISCUSSION OF 1-CHLORO-N-PHENYLALKANES

As in Fig. 4, we plot in Fig. 7 the peak DEA cross sections of the four compounds at both the (nominally)  $\pi_1^*$  and  $\sigma^*(\text{C}-\text{Cl})$  VAEs to compare with the cross section variation with VAE. The lines connecting the data points are again only to guide the eye. As the number of  $\text{CH}_2$  spacers increases, the cross section drops precipitously and the lower VAE, filled stars, approaches that of 1-phenylhexane (1.1 eV) shown at the position of the vertical dashed line. In contrast to the chloroalkenes in Fig. 4, the upper VAE, open stars, declines monotonically with the number of spacers, approaching that characteristic of long chain normal 1-chloroalkanes near 2.2–2.3 eV, but lying slightly above the

TABLE VIII. Peak DEA cross sections ( $\text{cm}^2$ ) and energies (eV) of the peaks in the 1-chloro-n-phenylalkanes.

Compound	Reference	Peak cross section	Peak energy
$\text{C}_6\text{H}_5-\text{CH}_2\text{Cl}$	Present work	$2.89 \times 10^{-16}$	0.54
	Ref. 6	$4.16 \times 10^{-16a}$	0.52
$\text{C}_6\text{H}_5-(\text{CH}_2)_2\text{Cl}$	Present work	$3.65 \times 10^{-17}$	0.75
	Ref. 6	$2.21 \times 10^{-17a}$	0.76
$\text{C}_6\text{H}_5-(\text{CH}_2)_3\text{Cl}$	Present work	$3.61 \times 10^{-18}$	0.92
	Ref. 7	$1.97 \times 10^{-18a}$	0.9
$\text{C}_6\text{H}_5-(\text{CH}_2)_4\text{Cl}$	Present work	$7.38 \times 10^{-19}$	0.82
	Ref. 7	$1.52 \times 10^{-18a}$	1.0

<sup>a</sup>Obtained from ratios normalized to a chlorobenzene DEA cross section of  $2.35 \times 10^{-17} \text{ cm}^2$ .

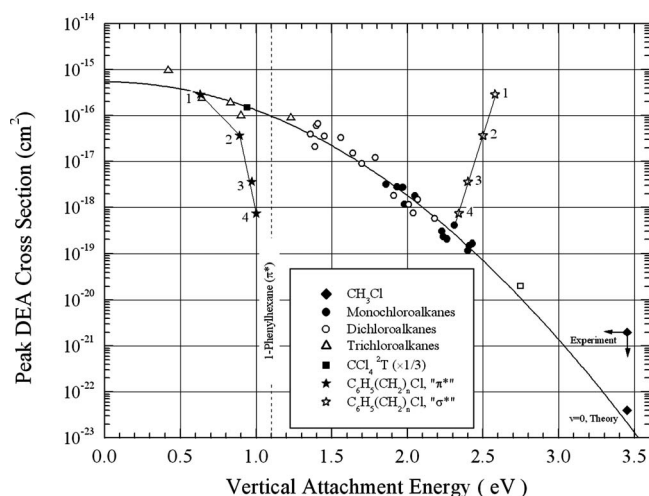


FIG. 7. As in Fig. 4 for the chlorophenylalkanes.

best fit line through the chloroalkane data, indicating that weak coupling between  $\pi^*$  and  $\sigma^*$  orbitals exists in the longest compound.

Modelli *et al.*<sup>7</sup> have noted earlier that the peak yields of  $\text{Cl}^-$  are higher in the phenyl derivatives than in the ethylenic compounds at each size of spacer unit. For the record, we find ratios of 1.4, 6.4, 4.8, and 1.8 for  $n=1-4$  respectively in this comparison. These authors have also suggested that contributions to DEA in the phenyl compounds may arise from temporary anion states associated with both  $\pi^*$  orbitals deriving from the degenerate  $e_{2u}$  orbitals of benzene. We suggest, however, that the difference arises mainly from the much lower  $\pi^*$  VAEs relative to those of the ethylenic compounds, which will give rise to longer resonance lifetimes. A calculation of the  $\pi_2^*$  MO of benzyl chloride, for example, shows that there is no direct overlap of  $\sigma^*(\text{C}-\text{Cl})$  with the phenyl  $\pi_2^*$  orbital wave function. Coupling would therefore have to arise by a different mechanism, namely, motion of Cl out of the plane perpendicular to the phenyl ring. The VAE was found to change very little with C–Cl angle.

Modelli *et al.*<sup>7</sup> have shown that, with the exception of benzyl chloride, the variation of the DEA cross sections with increasing spacer length tracks very well, over almost two orders of magnitude, the percentage of  $\sigma^*(\text{C}-\text{Cl})$  character of the LUMO computed with a simple Hückel type LCBO approach. Such a dependence indicates rather clearly the importance of the delocalization of the LUMO wave function over both  $\pi^*$  and  $\sigma^*$  moieties and is in contrast to the loosely phrased description sometimes encountered in the literature that suggests electron capture takes place into a localized  $\pi^*$  orbital with subsequent transfer to a localized  $\sigma^*$  site. The wave function coefficients play an important role in our treatment of remote bond breaking by interacting temporary anion states in the chloroethylenic series.<sup>11</sup> However, we found that it was necessary to account for the composite resonance lifetime as a function of these coefficients and their phases to successfully describe DEA in the full set of compounds that includes allyl chloride. We anticipate that a similar treatment will be required for the phenyl based compounds. Such a study is planned.

## ACKNOWLEDGMENTS

We thank Alberto Modelli for his comments on the manuscript.

- <sup>1</sup>K. Aflatooni and P. D. Burrow, *J. Chem. Phys.* **113**, 1455 (2000).
- <sup>2</sup>K. Aflatooni, G. A. Gallup, and P. D. Burrow, *J. Phys. Chem. A* **104**, 7359 (2000).
- <sup>3</sup>D. M. Pearl, P. D. Burrow, J. J. Nash, H. Morrison, and K. D. Jordan, *J. Am. Chem. Soc.* **115**, 9876 (1993).
- <sup>4</sup>D. M. Pearl, P. D. Burrow, J. J. Nash, H. Morrison, D. Nachtigallova, and K. D. Jordan, *J. Phys. Chem.* **99**, 12379 (1995).
- <sup>5</sup>T. Underwood-Lemons, G. Saghi-Szabo, J. A. Tossell, and J. H. Moore, *J. Chem. Phys.* **105**, 7896 (1996).
- <sup>6</sup>A. Modelli and M. Venuti, *J. Phys. Chem. A* **105**, 5836 (2001).
- <sup>7</sup>A. Modelli, M. Venuti, and L. Szepes, *J. Am. Chem. Soc.* **124**, 8498 (2002).
- <sup>8</sup>A. Modelli, *Phys. Chem. Chem. Phys.* **5**, 2923 (2003).
- <sup>9</sup>L. Sanche and G. J. Schulz, *Phys. Rev. A* **5**, 1672 (1972).
- <sup>10</sup>A. Modelli, *J. Phys. Chem. A* **109**, 6193 (2005).
- <sup>11</sup>P. D. Burrow and G. A. Gallup, *J. Chem. Phys.* **125**, 154309 (2006).
- <sup>12</sup>S. C. Chu and P. D. Burrow, *Chem. Phys. Lett.* **172**, 17 (1990).
- <sup>13</sup>A. Stamatovic and G. J. Schulz, *Rev. Sci. Instrum.* **41**, 423 (1970).
- <sup>14</sup>M. Guerra, D. Jones, G. Distefano, F. Scagnolari, and A. Modelli, *J. Chem. Phys.* **94**, 484 (1991).
- <sup>15</sup>D. M. Pearl and P. D. Burrow, *J. Chem. Phys.* **101**, 2940 (1994).
- <sup>16</sup>Our current VAE for allyl chloride supersedes an earlier value of 0.89 eV given by K. L. Stricklett, S. C. Chu, and P. D. Burrow, *Chem. Phys. Lett.* **131**, 279 (1986).
- <sup>17</sup>*A Handbook of Computational Chemistry*, T. Clark (Wiley-Interscience, New York, 1985).
- <sup>18</sup>T. Koopmans, *Physica (Amsterdam)* **1**, 104 (1934).
- <sup>19</sup>D. Chen and G. A. Gallup, *J. Chem. Phys.* **93**, 8893 (1990).
- <sup>20</sup>N. Heinrich, W. Koch, and G. Frenking, *Chem. Phys. Lett.* **124**, 20 (1986).
- <sup>21</sup>K. Aflatooni, G.A. Gallup, and P.D. Burrow, *J. Phys. Chem. A* **102**, 6205 (1998), the scaling differs slightly from the one in this reference, where geometry optimization with the 3-21G(d) basis set was used rather than 6-31G(d).
- <sup>22</sup>I. I. Fabrikant, *J. Phys. B* **27**, 4325 (1994); I. I. Fabrikant, personal communication.
- <sup>23</sup>G. Distefano, A. Modelli, M. Guerra, D. Jones, and S. Rossini, *J. Mol. Struct.* **174**, 177 (1988).